Study of the influence of computational parameters on the formation of a giant gaseous planet

Journal of Physics: Conference Series **641** (2015) 012012 doi:10.1088/1742-6596/641/1/012012

Study of the influence of computational parameters on the formation of a giant gaseous planet

R A Moraes[1] and E Vieira Neto[1]

[1]Universidade Estadual Paulista - UNESP - Campus de Guaratinguetá, SP, Brasil

E-mail: ricardo.moraes07@gmail.com

Abstract. Today, computational simulatios are the best method to describe the formation of our Solar System, however this kind of simulations contain numerical errors caused by boundary conditions and choises of the grid, for instance. In this paper we will present results from several hidrodynamical simulations of the formation of a planet like Jupiter able to migrate using different computational parameters. We will compare the density profile, the semimajor axis and the eccentricity of the planet for those different parameters and measure the effect of them. We will not extend our results for planets with initial eccentric orbits in this paper.

1. Introduction

One of the first hydrodynamical aproach for the formation of planets was given by [1], where the authors proposed a exponential model for the modeling of a gas nebula around the planet. Since there, with the advent of powerful computers it was developed a great number of computational facilities, which allow us to simulate with more accurate the formation of planets. Some examples are FARGO [5], ZEUS [8] and NIRVANA [10]. In [2] the authors compare the performance of several numerical integrators, including the ones cited here, in a simulation with two planets with mass comparable with Jupter and Neptune on circular orbits, the aim of the authors were invetigate the differences among the hydrodynamical codes and the reliability of the astrophysical hydrodynamic codes available at that time in the disk-planet problem, the authors was not interested in see the changes which appears when some numerical parameters are changed.

We will not perform simulations with many codes, but only with FARGO code, which the accurate is described in [5]. The pourpose of this paper is evaluate the effects of different parameters in a planet formation scenario, we will change the grid, the initial conditions, the accretion rate and the initial surface density (Σ_0).

This paper is organized as follows, in section 2 we describe the model set-up with all the parameters that was used, in the section 3 we presents the results of the simulations for the semimajor axis, eccentricity and density using different parameters and in the section 4 we draw our final conclusions about this work.

2. Numerical Model

In order to perform our hydrodymical simulations, we used the publically available FARGO (Fast Advection in Rotating Gaseous Objects). FARGO is by default a bidimentional hydrodynamical polar grid code centered on the star, based on the van Leer upwind algorithm on a staggered

mesh. It is capable to solves the Navier-Stokes and continuity equations for a Keplerian disk subject to the gravity of the central object and that of embedded protoplanets as well [9].

To simulate the gaseous nebula around planet we work with cilindrical coordinates (r, θ, z), with simetry on the z component with the vertically integrated equations. We adopted the viscous forces per unit of area of Navier-Stokes to model the viscous force. The origin of the coordenate system was placed on the central star, while the planet is at 1 dimensioless unity far from the star. The equations of motion and the gravitational potential are given by [4] or [7] and will not be repeated here.

We simulated a bidimensional protoplanetary disk. The tidal and viscous torque was considered, but the self-gravity was neglected. We work with an acretive disk, which has an inner radius of 0.4 and an outer radius of 2.5 with thickness radius given by the ratio $H/r = 0.05$. In addiction, all simulations was performed considering a planet with initial circular orbit with the aim to keep the problem as simple as possible.

2.1. Initial and Inner Boundary Conditions

In all simulations performed here we considered a corotating frame and the planet has the characteristics of Jupiter, its mass is $M_p = 10^{-3}\ M_*$, where M_* is the mass of the star and it is in a circular orbit around the star.

In this paper we use three different inner boundary conditions such as non-refleting, open and rigid. The outer boundary condition is open for all simulations, thus hereafter we will refer to the inner boundary connditions as boundary conditions. According to [5] the rigid boundary conditions, also know as wall boundary condition, is a low realistic condition and is often used to test codes, the use of this condition implies to set to zero the radial velocity at the boundary, besides the flow can not leave the mesh, which means that the gaseous mass will be conserved. On the other hand, we have the open boundary conditions, which allows the gas to move outside the mesh, in this case the total gaseous mass decrease with the time. For last, the non-reflecting boundary conditions are applied in order to eliminate the reflected waves on the planet, transporting these waves to a "ghost cell", improving the results, these boundary conditions does not restrict the disk to conserve its mass or angular momentum.

We will also analyze the density of the disk, for this we use different values for the initial density and the accretion rate. In hydrodynamic simulations of a planet we a mass of Jupiter it is usual to consider the initial density as 6.4×10^{-4} because this initial value means that theres the equivalent of two Jupiter masses in the disk interior to the orbital radius of the protoplanet [6], we will change this parameter ten times in order to see what kind of changes this increase in the initial density can produce. The same argumentation can be invoked to the accretion rate, for standart we will use 10^{-6} and in one simulation this value will be increased to 10^{-3}, which means that the planet will grow fastly, in theory the density of the gas might be lower in this simulation.

2.2. Grid

We work with a polar grid composed of radial and azimuthal (sectors) zones. The radial and azimuthal zones are both equally spaced, in particular, to use the FARGO algorithm we need to have equally spaced zones in the azimuth. The total number of cells in the mesh can be found using $N_t = N_{rad} \times N_{sec}$, where N_{rad} and N_{sec} are the number of radial and azimuthal zones, respectively. The number of cells are directly proportional to the accuracy of the results, which means that more cells in the mesh will given us better results.

In our simulations we used three meshes with different number of cells, 150×450, 300×300 and 300×900.

3. Simulations and Results

In this section we will describe the parameters of the simulations that was performed in this paper and our results.

In table 1 we show all the simulations and the most important parameters to our analysis. In addition, we are working on a corotating frame, with a planet in a circular orbit around the star, the planet was placed in one dimensionless unit and feel all disk effects, being able to migrate. The mass of the planet is the same for all simulations, even the ones which the accretion rate is different and all the simulations were performed for 300 Jupiter's orbits.

Table 1. List of simulations. Columns indicate: run abreviation (Name); mass of the planet; initial surface density; mass acretion rate; grid; inner boundary condition.

Name	$M_p\,(10^{-3}M_*)$	$\Sigma_0\,(10^{-4})$	$\dot{M}_p\,(10^{-6}M_*)$	Grid($N_{rad} \times N_{sec}$)	Boundary Condition
out.i.non	1	6.34	1	150×450	Non-reflecting
out.vii.non	1	6.34	1	300×300	Non-reflecting
out.iv.non	1	63.40	1	300×900	Non-reflecting
out.v.non	1	6.34	1000	300×900	Non-reflecting
out.vi.non	1	6.34	1	300×900	Non-reflecting
out.i.open	1	6.34	1	150×450	Open
out.i.rigid	1	6.34	1	150×450	Rigid

In the next topics we will analyze the influence of the boundary conditions, the grid, the accretion and the initial surface density analyzing the density profile, the semimajor axis and the eccentricty of the planet.

3.1. Boundary Conditions

In Figure 1 we show the density of the disk for the simulation with non-reflecting (out.i.non), open (out.i.open) and rigid (out.i.rigid) boundary conditions, respectively. As the profiles are similar, for a better interpretation of the results we can see in panel A of Figure 2 the comparison of the density of the disk in the planet for the same boundary conditions.

The Figure 2 shows the comparison of the disk density profile (panel A), semimajor axis (panel B) and eccentricty (panel C) for different inner boundary conditions.

In the panel A of the Figure 2 the density profile are shown, we can see that the distribution of gas is similiar for the non-reflecting and open conditions. However, when it was applied the rigid conditions we found a denser region inside and close to the planet, outside the planet the difference among the density profiles is small, which means that the densities of the gas converges to the same value far from the planet, independent of the boundary condition. Analyzing the panel B we can observe the behavior of the semimajor axis of the planet, as expected by the theory is possible identify an inner migration of the planet, once again for the non-reflecting and open boundary conditions the difference for the results are hardly noticed and for the rigid condition the planet migrates faster after 100 Jupiter's orbits, at this time a gap is opened by the planet. The panel C shows the evolution of the eccentricity of the planet, which starts circular. It is possible to see a small difference among the results, but once the behavior is the same for the three cases, the diferences are irrelevant.

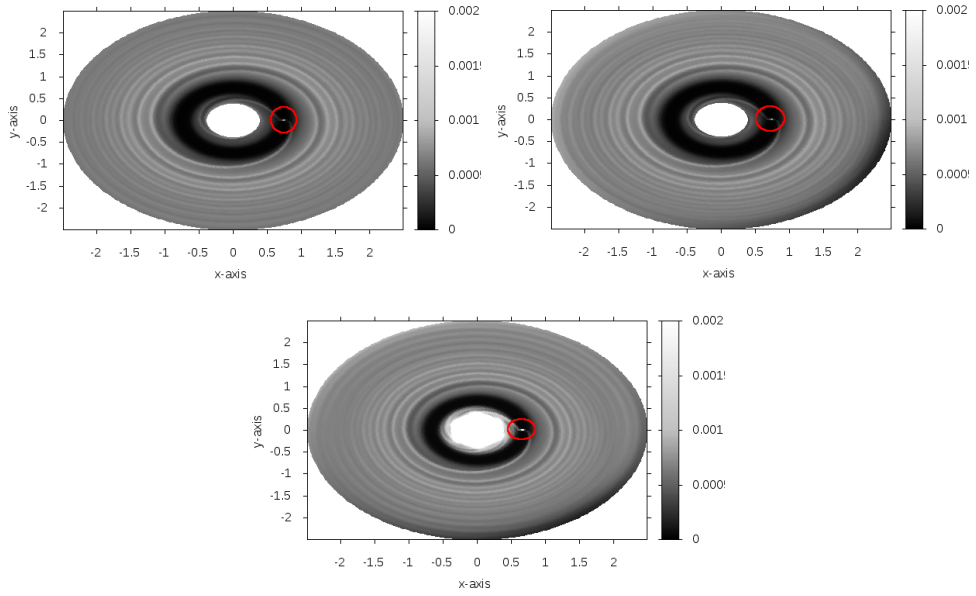

Figure 1. From the left to the right, density of disk for a simulation with non-reflecting, open and rigid boundary conditions, after 300 Jupiter's orbits. The red circle marks the location of the planet.

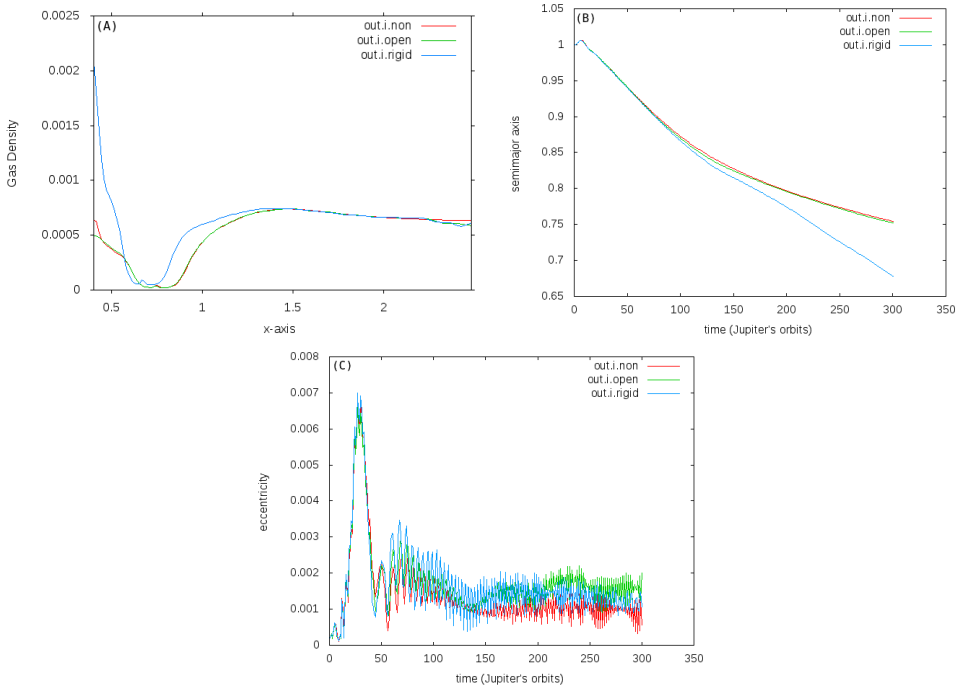

Figure 2. Comparison of the disk density profile (panel A), semimajor axis (panel B) and eccentricty (panel C) for non-reflecting (red line), open (green line) and rigid (blue line) boundary conditions after 300 Jupiter's orbits.

3.2. Grid

Figure 3 shows the comparison of the disk density profile (panel A), semimajor axis (panel B) and eccentricty (panel C) for different meshes. We used a low resolution grid, 150×450, with 67500 cells, an intermediate grid, 300×300, where the number of radial and azimuthal zones are equal, in this case the mesh have 90000 cells and a grid with higher resolution, 300×900, where the mesh have 270000 cells.

In practical terms we can say that a grid with more cells will give better results, because the number of cells is connected with the resolution of the results. On the other hand, more cells will produce more data to be processed, so the computational time will increase. All simulations discussed in the present topic was performed with non-reflecting boundary conditions due to its effcience to reproduce the formation of a planet [3].

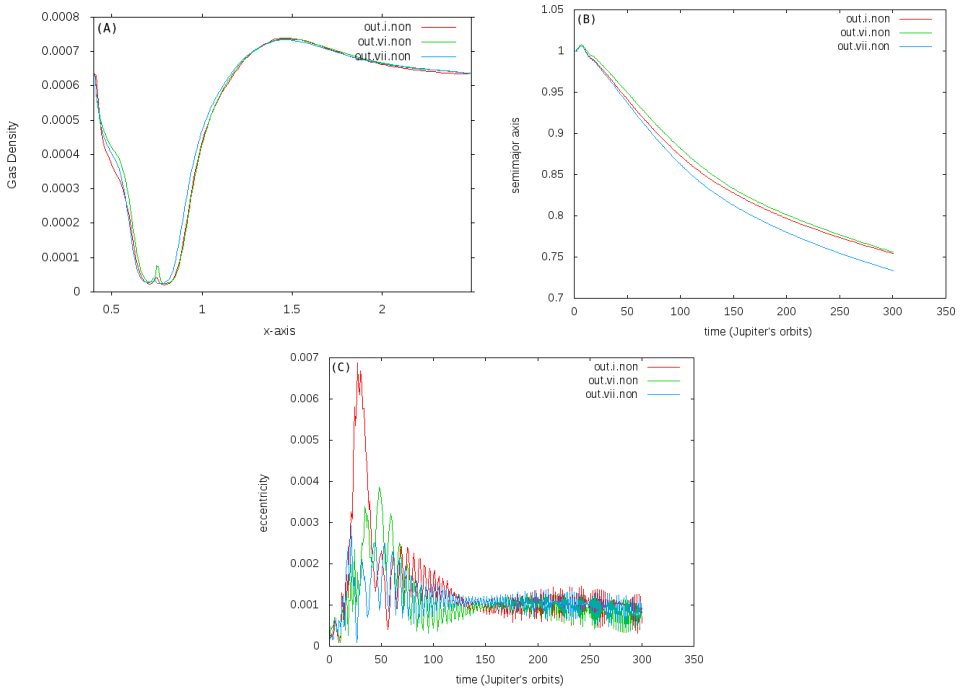

Figure 3. Comparison of the disk density profile (panel A), semimajor axis (panel B) and eccentricty (panel C) for three different grids: 150×450 (red line), 300×900 (green line) and 300×300 (blue line) after 300 Jupiter's orbits.

The simulation of the density profile (see panel A) shows that the profiles are slightly different, however, the grid with higher resolution (green line) the gas density around the planet has a peak compared with the other simulations, which means that the change grid has a strong influence over the results near the planet. The results for the semimajor axis are showed in panel B, the greatest variation between the simulations with the higher resolution (green line) and lower resolution (red line) appears around 100 Jupiter's orbits when the planet cleans its orbit opening a gap. This event starts on the vicinity of the planet, this may explain the difference of the results. The results of the simulation with a grid of 300×300 cells (blue line) may have been affected by the fact of the number of cells are equal, so the use of a grid with the same number of radial and azimuthal zones may not be a good choice. The panel C shows the comparison of the eccentricity among the three grids. The range of values reached by the simulations are not realy different, except for the simulation with the lower resolution which reaches a peak near 50

Jupiter's orbit with $e \approx 0.007$ while the simulation with higher resolution hits its top value at $e \approx 0.004$.

3.3. Accretion

The comparisons of the disk density profile (panel A), semimajor axis (panel B) and eccentricty (panel C) for two different accretion rates are shown in Figure 4. The goal is to see if the rate of amount of gas that the planet aggregates during its formation will interfere in the mentioned parameters.

Theoretically, the accretion rate will affect the time of formation of the planet, which will accumulates mass faster if the accretion rate is higher. However the discussion about how a different rate of gas being accreted will change the semimajor axis or the eccentricity of the planet was not discussed yet.

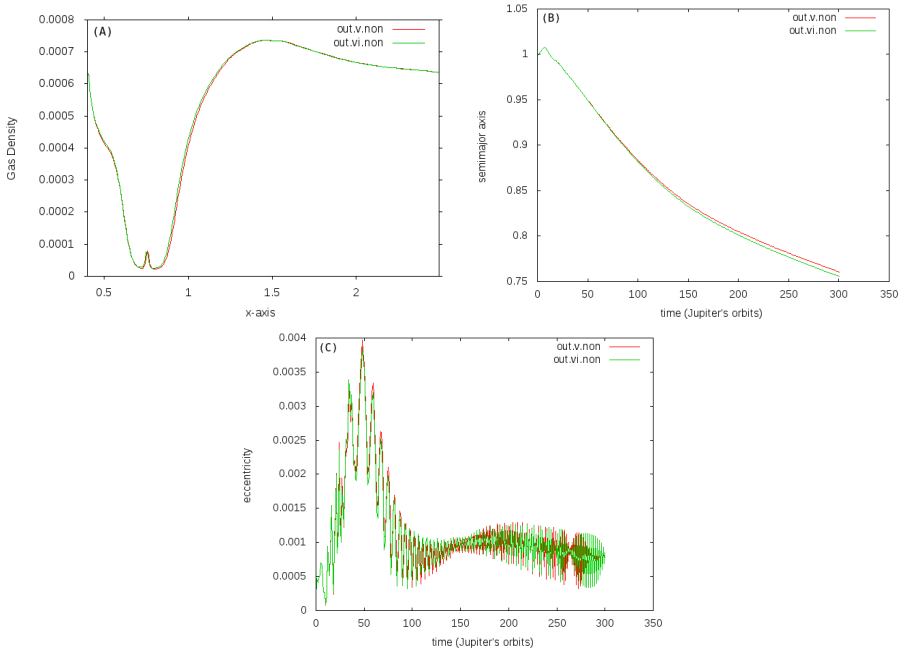

Figure 4. Comparison of the disk density profile (panel A), semimajor axis (panel B) and eccentricty (panel C) for two different accretion rates: $\dot{M}_p = 10^{-3}$ (red line) and $\dot{M}_p = 10^{-6}$ (green line) after 300 Jupiter's orbits.

Figure 4 shows that for all parameters studied here different accretion rates barely interfere in its behavior. In fact, the only variation that can be noticed appear in panel B, where it is possible to see that for a smaller acretion rate the planet migrates a slightly faster than the case with higher acretion rate.

3.4. Initial Surface Density

In this topic we analyze the disk density profile (panel A), semimajor axis (panel B) and eccentricty (panel C) for two initial surface density, the results are presented by Figure 5. The differents densities should alter all the disk structure and consequently the parameters of the planet.

Panel A of Figure 5 shows a result that was already expected, the density profile of the disk with greater initial density is denser than the profile of the disk with lower initial density. The

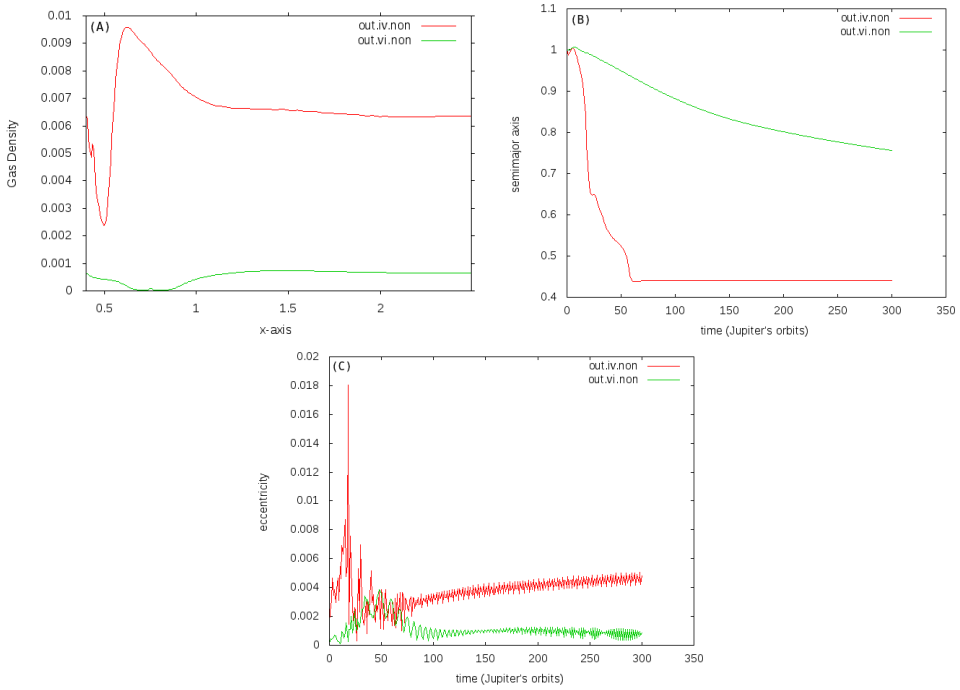

Figure 5. Comparison of the disk density profile (panel A), semimajor axis (panel B) and eccentricty (panel C) for two different initial surface density: $\Sigma_0 = 6.37 \times 10^{-3}$ (red line) and $\Sigma_0 = 3.67 \times 10^{-4}$ (green line) after 300 Jupiter's orbits.

main results are found for the semimajor axis and the eccentricity, panels B and C, respectively. For the denser disk, the semimajor axis decreases dramatically reaching the internal border of the disk immediately after 50 Jupiter's orbits. On the other hand, the eccentricity of the planet immersed in the denser disk increases moving away from values reached by the planet in the less dense disk, which means that the extra density brings disturbed effects for the disk.

4. Conclusion

For the three parameters evaluated the non-reflecting and the open boundary conditions does not change significantly the results, while the rigid boundary conditions have a denser density profile and the semimajor axis decreases faster, this happens mostly because on the rigid conditions scenario the gaseous mass is conserved.

The results for the grid show, as expected, that some effects close to the planet can be identified only with higher resolution, which leads us to say that the mesh with more cells is advised always that the aim of the simulation is study a small detailed region, also the option for the grid with the same number of radial and azimuthal zones presented poor results for the semimajor axis evolution.

For the parameters evaluated the change of the mass accretion rate does not shows significantly effect, so is possible to conclude that the accretion rate is not important for the density of the disk or for the evolution of the semimajor axis and eccentricty of the planet.

The simulations with two different initial densities was the one with more significantly contrast among the simulations performed in this paper, the result for the density of the disk was already expected, however, from the analysis of the semimajor axis and eccentricity we can conclude that the extra amount of gas in the disk drag the planet inside faster and bring

disturbed effects to the disk making the eccentricity of the planet grows.

Acknowledgments
The authors are thankful to the FAPESP, process number 2013/24281-9, for the financial support.

References

[1] Adachi I, Hayashi C and Nakazawa K 1976 *Progress of Theoretical Physics* **56** 1756
[2] de Val-Borro M *et al* 2006 *MNRAS* **370** 529
[3] Kley W 1999 *MNRAS* **303** 696
[4] Lubow S H, Seibert M and Artymowicz P 1999 *ApJ* **526** 1001
[5] Masset F 2000 *Astronomy and Astrophysics* **141** 165
[6] Nelson R P, Papaloizou J C B, Masset F, Kley W, 2000, *MNRAS* **318** 18
[7] Moraes R A and Vieira Neto 2013 *Journal of Physics: Conference Series* **465**
[8] Stone J, Norman M L 1992 *ApjS* **80** 753
[9] Zhang X, Liu B, Lin D N C and Li H 2014 *ApJ* **797** 20
[10] Ziegler U, Yorke H W 1997 *Comput. Phys. Commun.* **101** 54